

Structural, electronic, elastic, and thermal properties of $CaNiH_3$ perovskite obtained from first-principles calculations

S Benlamari, H Bendjeddou, R Boulechfar, S Amara Korba, H Meradji, R Ahmed, S Ghemid, R Khenata, S Bin Omran
Citation: Chin. Phys. B . 2018, 27(3): 037104. **doi:** 10.1088/1674-1056/27/3/037104

Journal homepage: http://cpb.iphy.ac.cn; http://iopscience.iop.org/cpb

What follows is a list of articles you may be interested in

Electronic and mechanical properties of half-metallic half-Heusler compounds CoCr*Z* (*Z*=S, Se, and Te)

Hai-Ming Huang(黄海铭), Chuan-Kun Zhang(张传坤), Ze-Dong He(贺泽东), Jun Zhang(张俊), Jun-Tao Yang(杨俊涛), Shi-Jun Luo(罗时军)
Chin. Phys. B . 2018, 27(1): 017103. **doi:** 10.1088/1674-1056/27/1/017103

First-principles investigation of the effects of strain on elastic, thermal, and optical properties of $CuGaTe_2$

Li Xue(薛丽), Yi-Ming Ren(任一鸣), Jun-Rong He(何俊荣), Si-Liu Xu(徐四六)
Chin. Phys. B . 2017, 26(6): 067103. **doi:** 10.1088/1674-1056/26/6/067103

Structural, elastic, and electronic properties of sodium atoms encapsulated type-I silicon-clathrate compound under high pressure

Zhang Wei, Chen Qing-Yun, Zeng Zhao-Yi, Cai Ling-Cang
Chin. Phys. B . 2015, 24(10): 107101. **doi:** 10.1088/1674-1056/24/10/107101

from first-principles calculations

Liu Qi-Jun, Zhang Ning-Chao, Liu Fu-Sheng, Liu Zheng-Tang
Chin. Phys. B . 2014, 23(4): 047101. **doi:** 10.1088/1674-1056/23/4/047101

First-principles investigation on the structural and elastic properties of *cubic*-Fe_2TiAl under high pressures

Liu Xian-Kun, Liu Cong, Zheng Zhou, Lan Xiao-Hua
Chin. Phys. B . 2013, 22(8): 087102. **doi:** 10.1088/1674-1056/22/8/087102

Structural, electronic, elastic, and thermal properties of $CaNiH_3$ perovskite obtained from first-principles calculations

S Benlamari[1], H Bendjeddou[1], R Boulechfar[1], S Amara Korba[1], H Meradji[1,†], R Ahmed[2], S Ghemid[1], R Khenata[3,‡], and S Bin Omran[4]

[1] *Laboratoire LPR, Département de Physique, Faculté des Sciences, Université Badji Mokhtar, Annaba, Algeria*
[2] *Department of Physics, Faculty of Science, Universiti Teknologi Malaysia, UTM, Skudai,* 81310 *Johor, Malaysia*
[3] *Laboratoire de Physique Quantique et de Modélisation Mathématique de la Matière (LPQ3M), Université de Mascara-*29000*-Algeria*
[4] *Department of Physics and Astronomy, College of Science, King Saud University, P.O. Box* 2455*, Riyadh* 11451*, Saudi Arabia*

(Received 27 October 2017; revised manuscript received 21 December 2017; published online 11 February 2018)

A theoretical study of the structural, elastic, electronic, mechanical, and thermal properties of the perovskite-type hydride $CaNiH_3$ is presented. This study is carried out via first-principles full potential (FP) linearized augmented plane wave plus local orbital (LAPW+lo) method designed within the density functional theory (DFT). To treat the exchange–correlation energy/potential for the total energy calculations, the local density approximation (LDA) of Perdew–Wang (PW) and the generalized gradient approximation (GGA) of Perdew–Burke–Ernzerhof (PBE) are used. The three independent elastic constants (C_{11}, C_{12}, and C_{44}) are calculated from the direct computation of the stresses generated by small strains. Besides, we report the variation of the elastic constants as a function of pressure as well. From the calculated elastic constants, the mechanical character of $CaNiH_3$ is predicted. Pertaining to the thermal properties, the Debye temperature is estimated from the average sound velocity. To further comprehend this compound, the quasi-harmonic Debye model is used to analyze the thermal properties. From the calculations, we find that the obtained results of the lattice constant (a_0), bulk modulus (B_0), and its pressure derivative (B'_0) are in good agreement with the available theoretical as well as experimental results. Similarly, the obtained electronic band structure demonstrates the metallic character of this perovskite-type hydride.

Keywords: perovskite-type hydrides, elastic constants, hydrogen storage materials

PACS: 71.15.Nc, 71.15.Mb, 71.15.Ap, 74.62.Fj **DOI:** 10.1088/1674-1056/27/3/037104

1. Introduction

In recent years, ternary hydrides ABH_3 have attracted considerable attention of a lot of scientists around the world because of their high hydrogen storage capacity and large number of other applications like switchable mirrors,[1–3] rechargeable batteries, energy storage, etc.[4,5] In ABH_3 ternary hydrides, A is usually an alkali or alkaline earth metal and B is a transition metal. Some of the ABH_3 ternary hydrides also show the perovskite-type structure in which H is regarded as the anion, and A and B are monovalent and divalent cations, respectively. If A is a heavier alkaline metal like Ca, Ba, Sr and B is Fe, Ni, or Co, the resultant ABH_3 compounds are reported stable, and this stability is associated with the filled d-band of the alkaline earth and transition metals. However, the priority to these hydrides is given mainly on the basis of their good storage capacities, good reversibility, and large reactivity.

The $CaNiH_3$ based alloys are expected to be attractive hydrogen storage materials in the coming hydrogen energy era because of their good hydrogenation properties and relatively low material cost. The perovskite-type hydride $CaNiH_3$ was discovered in the study of the decomposition of hydrogenated $CaNiH_3$ alloys in the H_2 atmosphere.[6] This ternary hydride has a large hydrogen content of 3 wt.% and decomposes to CaH_2 and Ni when it is heated from room temperature to 773 K in an H_2 atmosphere of 3 MPa. Some investigations have been reported in the literature.[6–9] The first work on the hydrogenation properties of $CaNiH_3$ was reported by Oesterreicher *et al.*[7] More recently, Takeshita *et al.*[6] reported the synthesis and decomposition of $CaNiH_3$ hydride at high temperatures up to 773 K, analyzed the hydrogenation properties and the change in crystal structure of $CaNiH_3$ by using differential thermal analysis (DTA) and x-ray diffraction (XRD). Sato *et al.* calculated its electronic band structures by employing the augmented plane wave method[8] and predicted the metallic nature of the $CaNiH_3$ compound. An experimental study of the formation and thermal desorption process of $CaNiH_3$ was also carried out.[9]

Although studies are reported on the hydrogenation/dehydrogenation processing, to the best of our knowledge, there are no experimental or theoretical data on the elastic, mechanical, and thermal properties of this interested compound, which are important to understand the real character of $CaNiH_3$ and its applicability for different applications. Thus the aim of this work is to give a comprehensive study on its physical properties by employing full potential (FP) linearized augmented plane wave plus local orbital (LAPW+lo) method

†Corresponding author. E-mail: hmeradji@yahoo.fr
‡Corresponding author. E-mail: Khenata_rabah@yahoo.fr
© 2018 Chinese Physical Society and IOP Publishing Ltd

framed within density functional theory (DFT) and implemented in the WIEN2k computational package. The organization of the rest of the paper is as follows. In Section 2, we briefly describe the methodology. In Section 3, we present and discuss the results of our study regarding the structural parameters, elastic constants, pressure dependence elastic constants, band structure, and thermal properties. Finally, in Section 4, we summarize the main conclusions of this work.

2. Calculation method

The first-principles calculations of this work are performed using the FP-LAPW+lo method[10] based on the DFT[11] as implemented in WIEN2k code.[12] In this approach, the crystal unit is partitioned into two regions: nonoverlapping muffin tin spheres (MT) and interstitial regions (IR). In the two regions, the Kohn Sham wave functions, charge density, and potential are treated differently. To determine the structural parameters, the local density approximation (LDA) of Perdew–Wang (PW)[13] and the generalized gradient approximation (GGA) of Perdew–Burke–Ernzerhof (PBE)[14] are employed. To avoid the overlapping, the muffin-tin radii ($R_{\rm MT}$) are taken to be 2.5, 2.03, and 1.10 for Ca, Ni, and H, respectively. To expand the charge density as well as the potential, the maximum angular moment $l_{\rm max} = 10$ is used inside the atomic spheres. To obtain the suitable total energy convergence in the interstitial regions, the basis functions are expanded to $R_{\rm MT}K_{\rm max} = 8.0$, where $K_{\rm max}$ is the maximum value of the wave vector K. The charge density is restricted to $G_{\rm max} = 14$ (Ryd)$^{1/2}$. The Brillouin zone integrations for the total energy are carried out using 35 special k-points in the irreducible part of the Brillouin zone. In order to investigate the thermal effects, Gibbs program based on the "quasi-harmonic Debye model" is used.[15]

3. Results and discussion

3.1. Structural properties

The $CaNiH_3$ ternary hydride, typically containing a single molecule, crystallizes in the perovskite-type cubic structure with $Pm\bar{3}m$ (#221) space-group. The Wyckoff positions of the atoms (Ca, Ni, and H) inside the unit cell are 1a (0,0,0), 1b (1/2,1/2,1/2), and 3c (1/2,0,0), respectively. In order to calculate the ground state properties of the $CaNiH_3$ hydride, the total energies are calculated for various volumes around the equilibrium position, and then the obtained results are fitted to the Murnaghan's equation of state.[16] The calculated total energy versus the unit cell volume of $CaNiH_3$ is shown in Fig. 1. The calculated lattice parameter a_0, bulk modulus B_0, and its first derivative B_0' for this ternary compound are listed in Table 1, together with the available experimental and other theoretical results. From Table 1, it is clear that our results are in good agreement with the previously reported experimental and theoretical results. Our calculated equilibrium lattice constants within the PBE-GGA (PW-LDA) are found just 0.39% (2.28%) lower than the experimental value,[6] indicating the reliability of our calculations. Our computed lattice constants are also in good agreement with those calculated by Sato *et al.*[8] Similarly, our predicted bulk modulus at the level of PBE-GGA is also somehow smaller than that obtained within PW-LDA. However, the bulk modulus obtained at the level of PW-LDA is consistent with the previously reported theoretical one.[8] On the whole, by comparing the results obtained at the levels of PBE-GGA and PW-LDA, we find that the results obtained for the structural parameters by PBE-GGA are improved over those by PW-LDA.

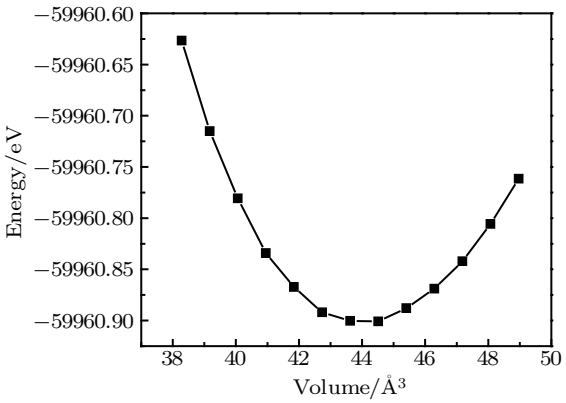


Fig. 1. Calculated total energy versus volume for $CaNiH_3$ using GGA approximation.

Table 1. Calculated lattice constant a_0, bulk modulus B_0, its pressure derivative B_0', and elastic constants C_{ij} for $CaNiH_3$ compared with other theoretical and experimental results.

Work	Method	a_0/Å	B_0/GPa	B_0'	C_{11}/GPa	C_{12}/GPa	C_{44}/GPa
Present	LDA	3.443	113.080[a]	4.279	186.13	76.54	59.28
			113.079[b]				
Present	GGA	3.530	94.223[a]	3.951	144.38	68.43	54.24
			93.752[b]	–	–	–	–
Exp.	–	3.544[6]	–	–	–	–	–
Other Calc.	GGA	3.526[8]	93.2[8]				

[a]From Murnaghan's equation of state.

[b]From $B_0 = (C_{11} + 2C_{12})/3$.

3.2. Elastic properties

The study of the elastic parameters is crucial to getting knowledge about the bonding among the nearest neighbors, structural stability, and anisotropic character of a material, and these parameters are vital to understanding the mechanical behavior. Moreover, studying the aforementioned parameters at the high pressure also provides information about the material response, mechanical stability, and strength under compression. As our system is cubic, it is well recognized that the three independent elastic constants are C_{11}, C_{12}, and C_{44}. To calculate the elastic constants, the Thomas Charpin method as integrated within the WIEN2k package is used[12] and the obtained elastic constants for the $CaNiH_3$ compound are given in Table 1. These are the first results concerning the elastic properties of this compound. From our calculations, we find that the calculated elastic constants C_{ij} are positive. The stability criteria for mechanical properties[17] are satisfied, that is, $(C_{11}-C_{12})>0$; $(C_{11}+2C_{12})>0$; $C_{11}>0$; $C_{44}>0$, alongside satisfying the bulk modulus B_0 criterion, i.e., $C_{12}<B_0<C_{11}$. From Table 1, one can easily see that the bulk modulus B_0 calculated from the elastic constants $B_0=\frac{1}{3}(C_{11}+2C_{12})$ has nearly the same value as the one obtained from the fitting of the data into the Murnaghan's equation of state (EOS). This might be an estimate of the reliability and accuracy of our predicted elastic constants for $CaNiH_3$. Furthermore from Table 1, it can also be noticed that the unidirectional compression found in terms of the elastic constant (C_{11}) in the principal crystallographic direction is much higher than that of C_{44}, demonstrating a weaker resistance to pure shear deformation in comparison with the resistance offered to unidirectional compression.

3.3. Mechanical properties

Knowledge of the elastic properties of materials promotes the understanding of the fundamental aspects of the mechanical deformation and structural properties of a crystal. In order to gain a deeper insight into the mechanical properties of the material, we calculate some polycrystalline elastic moduli such as the anisotropy factor A, Young's modulus E, Poisson's ratio υ, and shear modulus G by employing the Voigt Reus Hill approach and expressions given in the followings:[18–21]

$$A=\frac{2C_{44}}{C_{11}-C_{12}}, \tag{1}$$

$$E=\frac{9BG}{3B+G}, \tag{2}$$

$$\upsilon=\frac{3B-2G}{2(3B+G)}, \tag{3}$$

$$G=\frac{G_{\mathrm{R}}+G_{\mathrm{V}}}{2}, \tag{4}$$

where G_{R} is the representation of the Reuss's shear modulus related to the lower bound values of G, G_{V} is the representation of the Voight's shear modulus related to the upper bound values of G, which are respectively expressed as

$$G_{\mathrm{R}}=\frac{5C_{44}(C_{11}-C_{12})}{4C_{44}+3(C_{11}-C_{12})}, \tag{5}$$

$$G_{\mathrm{V}}=\frac{C_{11}-C_{12}+3C_{44}}{5}. \tag{6}$$

By using these relations, our calculated results are presented in Table 2. As Young's modulus E describes the hardness of a material, meaning that when the value is higher, the material is considered to be stiffer and exhibits covalent bonding.[22] The elastic anisotropy is another important physical quantity which tells about the structural stability and is decidedly coupled with the induction of the micro-cracks in the relevant material.[23] If the system is completely isotropic, then $A=2C_{44}/(C_{11}-C_{12})$ gives a value of unity, any deviation from this unity highlights its degree of elastic anisotropy. The computed A for $CaNiH_3$ is found to be 1.428 (1.082) using the PBE-GGA (PW-LDA), which means that our compound is not elastically completely isotropic. Similarly, another important factor is the ratio B/G which classifies the material's nature as ductile or brittle. Pugh's criterion[24] is used, i.e., if $B/G>1.75$, the material will be ductile, otherwise it will be of the brittle nature. By employing this criterion, one can observe from Table 2 that $CaNiH_3$ is a ductile material ($B/G=1.994$). Another index of ductility is Cauchy's pressure which is obtained by taking the difference, $C_{12}-C_{44}$. This difference serves as an indicator of ductility as well.[25] If $C_{12}-C_{44}$ for Cauchy's pressure is found to be positive (negative), the material is predicted to be of the ductile (brittle) nature. As the calculated results for the Cauchy's pressure of $CaNiH_3$ are positive, hence showing clearly that $CaNiH_3$ is of ductile nature. Poisson's ratio provides more information about the characteristic nature of the bonding forces. It has already been standardized that the values of of 0.5 and 0.25 are upper and lower limits of the Poisson's ratio, respectively, for the central force of a solid.[26] Following this, we see from Table 2 that the interactions in our investigated compound are central because the Poisson ratio is within the mentioned range.[27] Figure 2 displays the pressure dependence of the elastic constants and bulk moduli of $CaNiH_3$, which shows a linear dependence for all the plotted curves in the considered range of pressure. Also, we see that C_{11}, C_{12}, C_{44}, and B_0 increase with increasing pressure, and the elastic constant C_{11} is more sensitive to the change of pressure compared to the other elastic constants. To our knowledge, no experimental measurements or theoretical data for the elastic constants have been reported in the literature for this compound. This may give our results as a prediction for this hydride.

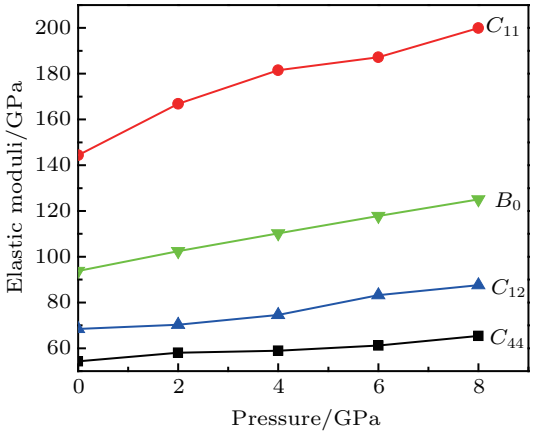


Fig. 2. (color online) Calculated pressure dependence of elastic constants C_{ij} and bulk modulus B_0 for $CaNiH_3$.

Table 2. Calculated density ρ, anisotropy factor A, Young's modulus E, Poisson's ratio υ, shear modulus G, (B/G) ratio, and Cauchy's pressure $C_{12}-C_{44}$ for $CaNiH_3$.

Method	ρ/g·cm^{-3}	A	E	υ	G	B/G	$C_{12}-C_{44}$
GGA	3.842	1.428	120.853	0.285	47.019	1.994	14.196
LDA	4.141	1.082	116.546	0.328	43.873	2.577	17.271

3.4. Debye temperature calculation

The role of the Debye temperature in the lattice vibration theory is the same as that of the Fermi temperature in the theory of electrons of metals since both represent a measure of the temperature to separate the low-temperature region (where quantum statistics is used) from the high temperature region (where classical statistics is found to be applicable). This is a very noteworthy parameter which is coupled to many materials' thermal characteristics, in turn correlating to a lot of their physical properties, for instance, elastic constants, specific heat, and melting temperature. Therefore, the knowledge of this parameter is essential for suggesting a material suitability for the electronic devices.

To calculate the Debye temperature θ_D, a typical technique is derived from the data of elastic constants in which θ_D is estimated by averaging sound velocity v_m by employing the equation[28]

$$\theta_D = \frac{h}{k_B}\left[\frac{3n}{4\pi}\left(\frac{N_A\rho}{M}\right)\right]^{1/3} v_m, \tag{7}$$

where k_B, h, and ρ denote Boltzmann's constant, Plank's constant, and the density, respectively. N_A is Avogadro's number, n is the number of atoms in a molecule, and M is the molecular weight.

To calculate the average sound velocity, the following relation is used:

$$v_m = \left[\frac{1}{3}\left(\frac{2}{v_t^3}+\frac{1}{v_l^3}\right)\right]^{1/3}, \tag{8}$$

where v_t and v_l are the transverse and longitudinal sound velocities, respectively. These values are obtained using Navier's equation[29]

$$v_l = \left(\frac{B+0.75G}{\rho}\right)^{1/2}, \tag{9}$$

$$v_t = \left(\frac{G}{\rho}\right)^{1/2}. \tag{10}$$

Our calculated results of θ_D, (v_t, v_l, v_m), and ρ of $CaNiH_3$ employing relations (7)–(10) are tabulated in Table 3. It is found that the longitudinal velocity has a larger value as compared to the above-described velocities because the particle displacement is parallel to the direction of the wave propagation in longitudinal wave. Like the elastic constants, to our knowledge, no prediction or experimental investigation is found yet in the reported literature for comparison. It is expected that future experiments will confirm our reported calculations.

Table 3. Calculated longitudinal v_l, transverse v_t, average elastic wave velocities v_m, and Debye temperature θ_D for $CaNiH_3$.

Method	v_l/m·s^{-1}	v_t/m·s^{-1}	v_m/m·s^{-1}	θ_D/K
GGA	6381.176	3498.307	3900.308	562.55
LDA	6436.889	3254.962	3649.013	539.62

3.5. Electronic properties

The calculated band structure of the perovskite-type hydride $CaNiH_3$ along the higher symmetry directions in the Brillouin zone using (PBE-GGA) approach is shown in Fig. 3. The Fermi level is set at zero energy. From this figure, it can be seen that there are some bands that cross E_F, indicating the metallic chiastic of $CaNiH_3$. For obtaining deeper insight into the electronic structure of $CaNiH_3$, the total and partial densities of states (TDOS and PDOS) are displayed in Fig. 4. The lowest valence band in the energy range from -10.0 eV to -6.0 eV below E_F is found mainly due to the Ni-s and H-s states with a few contribution from the Ca-s states. The narrow band between -6.5 eV and -5.5 eV is the doubly degenerate level, which is mainly originated from the Ni-d_{eg} states and is in fact responsible for the bonding of Ni–H. The non-binding, triplet degenerate Ni-d t2g states are also found to appear at -2.5 eV. At high energies, from -1.5 eV to 1.5 eV, the doubly degenerate state at the Γ point is an antibonding combination of Ni-d_{eg} and H-s states with Ca-d hybridization, resulting in the only half filling of the band. This half-filled band makes the $CaNiH_3$ a metallic conductor. The calculated DOS at E_F is around 0.865 states/eV/ atom. These states are mainly the d states of the Ni atoms. However, it is clear from Fig. 4 that there is very small contribution of Ca atomic states to the bands below the Fermi level. Overall the density of states profile and band structure plots are seen almost similar. Our obtained band structures are also found to be comparable with the already reported one by Sato *et al.*[8] The authors also predicted that $CaNiH_3$ is characterized as a metallic conductor.

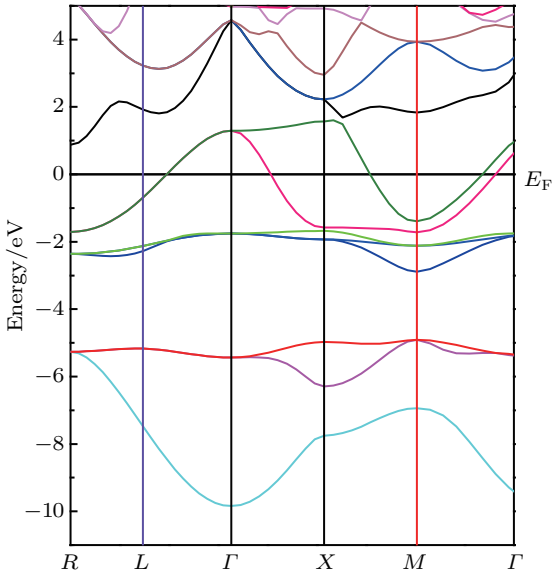


Fig. 3. (color online) Band structure alone high-symmetry directions in the Brillouin zone for the $CaNiH_3$ compound.

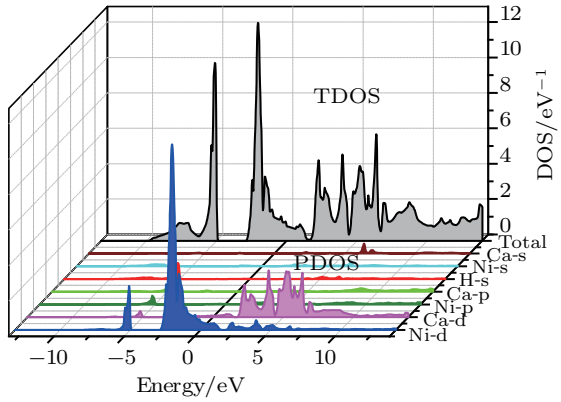


Fig. 4. (color online) Calculated total and partial densities of states for the $CaNiH_3$ compound.

3.6. Thermal properties

In order to determine the thermal effects at high pressure and high temperature, Gibbs computational code based on the quasi-harmonic Debye model is used.[30] In this method, Gibbs function $G^*(V;P,T)$ in the non-equilibrium form is described in the following way:

$$G^*(V,P,T) = E(V) + PV + A_{\text{vib}}, \tag{11}$$

where G^* is the non-equilibrium Gibbs function, $E(V)$ is the total energy/unit cell, the product PV stands for the constant hydrostatic pressure condition, and vibrational Helmholtz free energy A_{vib} and is written as[31,32]

$$A_{\text{vib}}(\theta;T) = nk_{\text{B}}T\left[\frac{9\theta}{8T} + 3\ln\left(1-\mathrm{e}^{-\theta/T}\right) - D\left(\frac{\theta}{T}\right)\right]. \tag{12}$$

Here, $D(\theta/T)$ is the Debye integral for an isotropic solid, and n is the number of atoms/formula unit. The expression for θ_{D} is given as[31]

$$\theta_{\text{D}} = \frac{\hbar}{k_{\text{B}}}\left[\left(6\pi^2 V^{1/2} n\right)\right]^{1/3} f(\sigma)\sqrt{\frac{B_{\text{s}}}{M}}, \tag{13}$$

where M is the molecular mass per unit cell and B_{s} is the adiabatic bulk modulus in the Debye model, which is approximated by the static compressibility as follows:[30]

$$B_{\text{s}} \cong B(V) = V\left\{\frac{\mathrm{d}^2E(V)}{\mathrm{d}V^2}\right\}. \tag{14}$$

The comprehensive description of the function $f(\sigma)$ can be seen in Refs. [33] and [34]; σ is the Poisson ratio which takes the value 0.25.[35] The Gibbs function $G^*(V,P,T)$, which is a function of (V,P,T), for non equilibrium conditions is minimized with regard to volume V as

$$\left[\frac{\partial G^*(V,P,T)}{\partial V}\right]_{P,T} = 0. \tag{15}$$

From the solution of Eq. (15), one can derive the corresponding thermal equation of state $V(P,T)$. From this, the heat capacity (C_V), isothermal bulk modulus (B_T), and the coefficients of the thermal expansion (α) can be obtained as[36]

$$B_T(P,V) = V\left(\frac{\delta^2 G^*(V;P,T)}{\delta V^2}\right)_{P,T}, \tag{16}$$

$$C_V = 3nk_{\text{B}}\left[4D\left(\frac{\theta}{T}\right) - \frac{3\theta/T}{\mathrm{e}^{\theta/T}-1}\right], \tag{17}$$

$$\alpha = \frac{\gamma C_V}{B_T V}, \tag{18}$$

where γ is the Grüneisen parameter, which is defined as

$$\gamma = -\frac{\mathrm{d}\ln\theta(V)}{\mathrm{d}\ln V}. \tag{19}$$

In the present study, the calculations of the thermal properties are done over a temperature range from 0 to 600 K. It is found that the quasi-harmonic model is most likely applicable in view of the fact that the temperature we considered is far away from the melting temperature. The pressure effects are investigated over a range of 0–6 GPa. Figure 5 presents the lattice parameters of the $CaNiH_3$-perovskite under different pressures at different temperature. One can easily note that the lattice parameters increase with increasing temperature at a given pressure, however, the increasing rate is very modest. The lattice constants dramatically decrease with increasing pressure at a given temperature. The temperature effect on the bulk modulus is shown in Fig. 6. It can be seen from the figure that the obtained bulk moduli are almost constant from 0 to 100 K, but decrease linearly above 100 K. It is also found that the compressibility decreases with increasing pressure at a given temperature and increases with increasing temperature at a given pressure owing to the fact that the effect of decreasing temperature is same as that of increasing pressure on the material. The specific heat is another important thermodynamic property of the material which measures

the loss ability or heat retention. Moreover, it provides the insight into the vibrational and many other obligatory properties of a substance. We plot the heat capacities C_V and C_P versus temperature at various pressures in Figs. 7(a) and 7(b). As it can be seen in these figures that at low-temperature ($T < 100$ K), C_V and C_P increase more rapidly with increasing temperature and then C_V becomes proportional to T^3.[37] Comparing $C_V(T)$ for different pressures, one can deduce that the influence of the pressure on $C_V(T)$ is significant at low temperature ($T < 100$ K), whereas at high temperature, the effect of the pressure on the variation of $C_V(T)$ with temperature becomes smaller and the heat capacity at constant volume calculated at each pressure tends to approach the Petit and Dulong limit (123 J·mol^{-1}·k^{-1}) similar to most of solids.[38] At high temperature, C_P continues to increase linearly. But, for the intermediate temperature range, it is found that the specific heat capacity is mainly governed by the atomic vibrations. The calculated C_V and C_P at room temperature (300 K) and zero pressure are 104.553 J·mol^{-1}·K^{-1} and 105.460 J·mol^{-1}·K^{-1}, respectively.

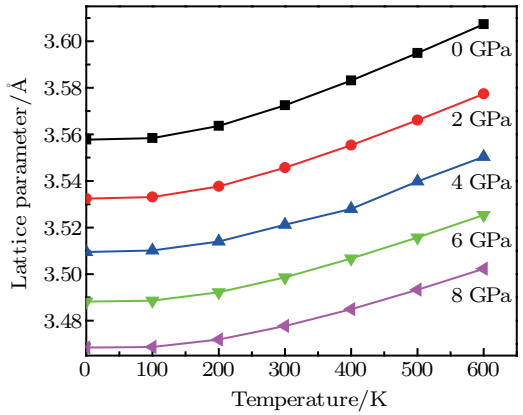


Fig. 5. (color online) Variation of the lattice constant as a function of temperature at different pressures for $CaNiH_3$.

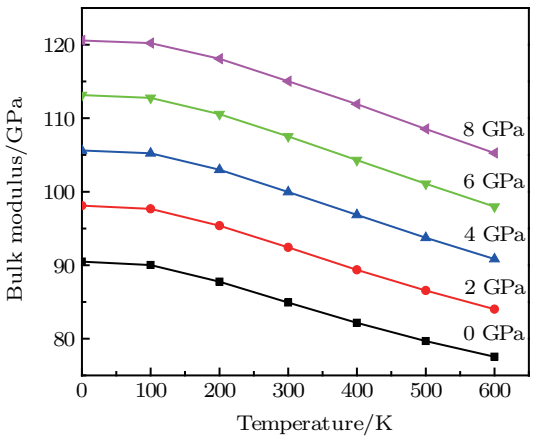


Fig. 6. (color online) Variation of the bulk modulus as a function of temperature at different pressures for $CaNiH_3$.

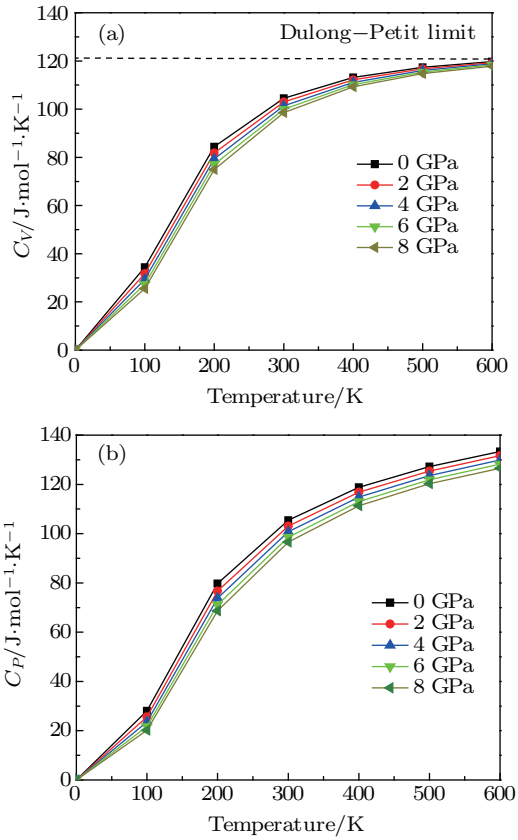


Fig. 7. (color online) Variation of the heat capacities (a) C_V and (b) C_P versus temperature at various pressures.

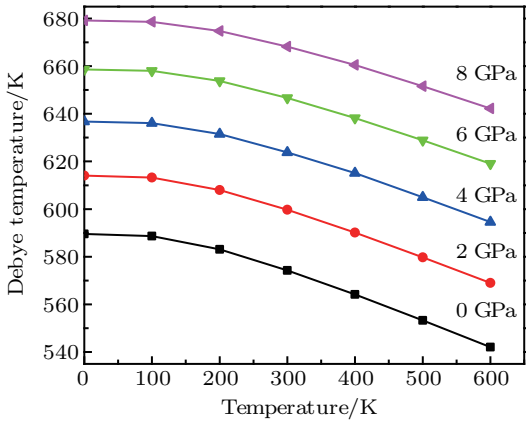


Fig. 8. (color online) Variation of the Debye temperature θ_D with the temperature at different pressures for $CaNiH_3$.

The variation of the Debye temperature with respect to the pressure is presented in Fig. 8. From the figure, one can easily note that θ_D is almost constant within the temperature range from 0 to 100 K and starts decreasing linearly with the increase of the temperature above 100 K. We also note that with the constant temperature, θ_D approximately increases linearly with respect to the applied pressure. Thus the temperature/pressure dependence of θ_D clearly shows that the atomic thermal vibrational frequency of the $CaNiH_3$ hydride varies with the temperature and pressure. As it is recognized already that the harder materials demonstrate higher θ_D. It is obvious

from Fig. 8 that the θ_D with regard to the pressure confirms the positive trend. From our calculations, we find that the θ_D at room temperature and zero pressure is 574.65 K. We also find that our obtained results are in nice agreement with the obtained results by following the relations of the sound velocities, i.e., 562.55 K. Our work regarding C_V and θ_D is the first attempt about this material as there is no study found in the literature. Hence our work might be the first attempt in this direction.

4. Conclusion

The calculations of the structural, elastic, thermal, and electronic properties of the $CaNiH_3$ ternary compound were carried out by using *ab initio* FP-LAPW+lo computational method at the level of PW-LDA and PBE-GGA exchange–correlation energy functional. We found that the obtained results of the lattice constants, as well as bulk modulus, were in a nice agreement with the available data in the literature. Also, we have computed elastic constants C_{11}, C_{12}, and C_{44} to determine the shear modulus, anisotropy factor, and Debye temperature. It was found that our computed elastic constants of $CaNiH_3$ adequately followed the stability criteria whereas its electronic band structure and DOS profile demonstrated its metallic nature. To understand the dependence of the lattice parameters, bulk modulus, Debye temperature, and specific heat capacity on the temperature and pressure, the quasi-harmonic Debye model was employed. It was deduced that our predictions concerning specific heat C_V of the $CaNiH_3$ hydride were closely following the Dulong–Petit law, showing that our results were in line with many other solids at high temperature. Hence, our first-principles DFT calculations performed in this study can be a very useful as a guide to complement future experiments.

Acknowledgement

The authors (Khenata and Bin-Omran) extend their sincere appreciation to the Deanship of Scientific Research at King Saud University for funding the Prolific Research Group (PRG-1437-39).

References

[1] Huiberts J N, Griessen R, Rector J H, Wijngaarden R J, Dekker J P, de Groot D G and Koeman N J 1996 *Nature* **380** 231
[2] Den Broeder F J A, Van der Molen S J, Kremers M, Huiberts J N, Nagengast D G, van Gogh A T M, Huisman W H, Koeman N J, Dam B, Rector J H, Plota S, Haaksma M, Hanzen R M N, Jungblut R M, Duine P A and Griessen R 1998 *Nature* **394** 656
[3] Kerssemakers J W J, van der Molen S J, Koeman N J, Günther R and Griessen R 2000 *Nature* **406** 489
[4] Chen P, Xiong Z T, Luo J Z, Lin J and Lee Tan K 2002 *Nature* **420** 302
[5] Schlapbach L and Züttel A 2001 *Nature* **414** 353
[6] Takeshitaa H T, Oishi T and Kuriyama N 2002 *Alloys Compd.* **333** 266
[7] Oesterreicher H, Ensslen K, Kerlin A and Bucher E 1980 *Mater. Res. Bull.* **15** 275
[8] Sato T, Noréus D, Takeshita H and Häussermann U 2005 *Sol. Stat. Chem.* **178** 3381
[9] Ikeda K, Kato S, Ohoyama K, Nakamori Y, Takeshita H T and Orimo S 2006 *Scr. Mater.* **55** 827
[10] Koelling D D and Harmon B N 1977 *Phys. C: Sol. Stat. Phys.* **10** 3107
[11] Hohenberg P and Kohn W 1964 *Phys. Rev. B* **136** 864
[12] Blaha P, Schwarz K, Madsen G K H, Kvasnicka D and Luitz J 2001 WIEN2k. *An Augmented Plane Wave + Local Orbitals Program for Calculating Crystal Properties,* Vienna University of Technology, Vienna, Austria
[13] Perdew J P and Wang Y 1992 *Phys. Rev. B* **45** 13244
[14] Perdew J P, Burke K and Ernzerlof M 1996 *Phy. Rev. Lett.* **77** 3865
[15] Blanco M A, Francisco E and Luaña V 2004 *Comput. Phys. Commun.* **158** 57
[16] Murnaghan F D 1944 *Proc. Natl. Acad. Sci. USA* **30** 244
[17] Grimvall G 1999 *Thermophysical Properties of Materials* (Amsterdam: Elsevier)
[18] Voigt W 1928 *Lehrbuch der Kristallphysik*, Taubner, Leipzig
[19] Russ A and Angew A 1929 *Mater. Phys.* **9** 49
[20] Wu Z J, Zhao E J, Xiang H P, Hao X F and Liu X J 2007 *Phys. Rev. B* **76** 054111
[21] Peng F, Chen D, Fu H and Cheng X 2009 *Phys. Status Solidi B* **246** 71
[22] Jenkins C H and Khanna S K 2005 *Mech. Mater.* **62** 16
[23] Tvergaard V and Hutshinson J W 1988 *J. Am. Ceram. Soc.* **71** 157
[24] Pugh S F 1954 *Philos. Mag.* **45** 823
[25] Pettifor D G 1992 *Mater. Sci. Technol.* **8** 345
[26] Fu H, Li D, Peng F, Gao T and Cheng X 2008 *Comput. Mater. Sci.* **44** 774
[27] Ma X G, Liang P, Miao L, Bie S W, Zhang C K, Xu L and Jiang J J 2009 *Phys. Status Solidi B* **246** 2132
[28] Johnston I, Keeler G, Rollins R and Spicklemire S 1996 *Solid State Physics Simulations, The Consortium for Upper-Level Physics Software* (New York: Jhon Wiley)
[29] Schreiber E, Anderson O L and Soga N 1973 *Elastic Constants and their Measurements* (New York: McGraw-Hill)
[30] Blanco M A, Francisco E and Luaña V 2004 *Comput. Phys. Commun.* **158** 57
[31] Blanco M A, Martín Pendás A, Francisco E, Recio J M and Franco R 1996 *Mol. Struct. Theochem.* **368** 245
[32] Flórez M, Recio J M, Francisco E, Blanco M A and Martín Pendás A 2002 *Phys. Rev. B* **66** 144112
[33] Francisco E, Recio J M, Blanco M A and Martin Pendas A 1998 *Phys. Chem.* **102** 1595
[34] Francisco E, Blanco M A and Sanjurio G 2001 *Phys. Rev. B* **63** 094107
[35] Poirier J P 2000 *Introduction to the Physics of the Earth's Interior* (Cambridge Cambridge University Press)
[36] Hill R 1952 *Proc. Phys. Soc. Lond. A* **65** 349
[37] Petit A T and Dulong P L 1819 *Ann. Chim. Phys.* **10** 395
[38] Debye P 1912 *Ann. Phys.* **39** 789